Structural and Morphological Characterisation of CdS: In Thin Films Grown by Spin Coating Method

Ogechi Ogana John[1], Daniel Ketui1, Duke Oeba[2]

[1]Department of physics: faculty of science, Kisii University P.o box 408-40200, Kisii, Kenya

[2]Department of physics, faculty of science, Egerton University, p.o box 536-20115, Egerton Kenya

***Corresponding author**

ABSTRACT

A photovoltaic cell, or solar cell, is a device that converts light energy into electrical energy through the photovoltaic effect. these cells are fabricated from light-absorbing materials which, upon illumination, generate charge carriers that produce an electric current. to evaluate the suitability of a material for photovoltaic applications, it is essential to investigate its structural and morphological properties under operational conditions. This paper focuses on the preparation and characterization of indium-doped cadmium sulfide (CdS:In) thin films as window materials for thin-film photovoltaic cells. the films were deposited using the spin coating technique followed by thermal annealing to enhance their structural integrity and surface properties. the CdS thin films were found to exhibit a hexagonal crystal structure with an average crystallite size of 13.44 nm. morphological analysis revealed improved surface uniformity and grain distribution with increased indium doping. these results indicate that indium incorporation enhances the crystallinity and surface morphology of CdS thin films, making them more suitable for photovoltaic applications.

Key words: Thin films, structural and morphological properties

INTRODUCTION

The increasing global demand for sustainable and cost-efficient energy solutions has significantly accelerated advancements in thin-film photovoltaic technologies(Wilson et al., 2020) . Thin films play a crucial role in solar cell development due to their ability to minimize material consumption while enabling controlled structural engineering at the nanoscale (Luo et al., 2016). Among the various materials investigated for window layer applications, cadmium sulfide (CdS) remains one of the most widely studied due to its favorable structural characteristics and compatibility with diverse heterojunction systems (Wahab et al., 2026).

The crystalline phase, grain size, and orientation of CdS thin films are critical factors that influence charge transport mechanisms, defect density, and interfacial properties in photovoltaic devices (Kumari et al., 2025).Structural uniformity and phase purity are particularly important in ensuring consistent electrical pathways and minimizing recombination centers within the material.

CdS has gained widespread application as a window layer material in thin-film solar cells and is commonly integrated with absorber layers such as CdTe (S. G. Kumar & Rao, 2013), $CuInGaSe_2$ (Raza, 2025), CuO (Hossain et al., 2020), PbS (Xu et al., 2022), Cu_2ZnSnS_4 (Yasin et al., 2026), SnS (Yasin et al., 2026), and ZnS (Madhavi & Prasad, 2020). This compatibility is largely attributed to its stable crystalline framework and its ability to form well-defined interfaces with a variety of absorber materials . Compared to alternative window materials, CdS exhibits reliable chemical stability and structural integrity under different processing conditions, making it suitable for scalable device fabrication.

The structural properties of CdS can be significantly modified through substitutional doping. Incorporation of dopant elements into the CdS lattice introduces lattice distortions, alters grain growth dynamics, and influences crystallite size and orientation . In particular, doping with trivalent elements such as indium (In^{3+}) leads to substitution of Cd^{2+} ions within the lattice, resulting in localized strain due to differences in ionic radii and valence states. These effects can enhance crystallinity and promote grain boundary modification, leading to improved film compactness and reduced defect-related imperfections.

In this investigation, indium was introduced as a dopant at concentrations of 0.005 M, 0.007 M, 0.009 M, and 0.011 M for samples labeled SA, SB, SC, and SD, respectively. The variation in dopant concentration plays a significant role in determining nucleation and growth mechanisms during film formation. At lower concentrations, incomplete grain coalescence may occur, leading to non-uniform surface morphology. As the dopant concentration increases, enhanced nucleation rates promote the formation of more compact and continuous films. However, excessively high doping levels may introduce lattice strain and defect clustering, which can adversely affect structural stability.

Various deposition techniques have been employed in the synthesis of CdS thin films, including chemical bath deposition (CBD) (Madhavi & Prasad, 2020), thermal evaporation (Lakmal et al., 2021), pulsed laser deposition (PLD) (Belaid et al., 2024), sputtering (Das et al., 2020), atomic layer deposition (ALD), (Johnson et al., 2014) physical vapor deposition (Johnson et al., 2014), spray pyrolysis (Shkir et al., 2020), molecular beam epitaxy (Li et al., 2023), close space sublimation (Huang et al., 2026), successive ionic layer adsorption (Deshmukh et al., 2018) and reaction (SILAR), screen printing(V. Kumar et al., 2011), and spin coating . While many of these techniques produce high-quality films with controlled crystallinity, they often involve complex procedures and high operational costs. In contrast, spin coating has emerged as a simple, cost-effective, and scalable technique for fabricating uniform thin films.

The spin coating process involves the deposition of a precursor solution onto a substrate, followed by rapid rotation to spread the solution evenly through centrifugal force. This technique enables fine control over film thickness and uniformity by adjusting parameters such as solution viscosity, spin speed, and annealing conditions. Post-deposition thermal treatment plays a critical role in improving crystallinity, facilitating grain growth, and eliminating residual stresses within the films.

X-ray diffraction (XRD) analysis conducted in this study confirmed that all deposited films retained a pure hexagonal CdS phase, indicating that indium doping did not alter the fundamental crystal structure(Shkir et al., 2019). The diffraction patterns exhibited well-defined peaks corresponding to preferred crystallographic orientations, suggesting improved crystallinity with increasing dopant concentration. The enhancement in peak intensity observed at higher doping levels indicates larger crystallite sizes and reduced structural disorder (Sen et al., 2020).

Scanning Electron Microscopy (SEM) analysis further revealed that the films exhibited a compact and uniformly distributed grain structure. The surface morphology showed significant improvement with increasing indium concentration, transitioning from relatively coarse and irregular grain formations to smoother and more densely packed structures. This morphological evolution is indicative of enhanced grain boundary connectivity, which is essential for efficient charge transport in device applications. Uniform grain distribution also minimizes the presence of voids and pinholes, thereby improving the overall structural integrity of the films (Jothika et al., 2025).

Although extensive research has been conducted on CdS thin films, this study emphasizes the importance of optimizing dopant concentration to achieve desirable structural and morphological characteristics. Controlled indium incorporation has been shown to significantly influence crystal growth behavior, grain size distribution, and surface uniformity. These structural improvements are critical in addressing limitations associated with defect formation and poor film continuity in thin-film photovoltaic devices (Dong et al., 2026).

By focusing on spin coating and controlled indium doping, this work contributes to the advancement of structurally optimized CdS thin films for application in photovoltaic systems. Future studies should explore the long-term structural stability of these films under operational conditions, as well as investigate the correlation between microstructural evolution and device performance. Such investigations will further support the development of robust and scalable thin-film technologies for next-generation solar energy applications (Arun et al., 2025).

METHODOLOGY

Materials Required

Cadmium nitrate tetrahydrate [$Cd(NO_3)_2 \cdot 4H_2O$] (99.95%)-sigma Aldrich, indium nitrate hydrate [$In(NO_3)_3 \cdot xH_2O$] (99.99%)- sigma Aldrich, thiourea [$(NH_2)_2CS$] (99.95 %) -sigma Aldrich, ammonium nitrate [NH_4NO_3] (99.98 %)- sigma Aldrich and distilled water (solvent).

Cleaning of Substrate

The glass substrates coated with fluorine-doped tin oxide (FTO) were cleaned by wiping their surface with dust-free wipes dipped in a solvent of acetone and then dried. The wipes were used to remove dust, fingerprints and all kinds of organic contaminants including grease and oil. They were then further cleaned with ethanol to remove any residual impurities. Substrates were then thoroughly washed with the deionized water to remove traces of solvents. After cleaning the substrates were dried in a vacuum oven at 60°C to prevent damage to the conductive coating and were left to cool and dry for about 10 minutes. Lastly, the substrates were removed and kept in a dusty free setting before using them.

Deposition of Indium-Doped Cadmium Sulfide (CdS:In) Thin Films

Cadmium nitrate tetrahydrate was dissolved in distilled water to make a 0.1 M cadmium nitrate solution. A 0.15 g of indium nitrate hydrate in 100 ml of distilled water was taken out for preparation of a 0.005 M solution of indium nitrate. A solution of 0.2 M thiourea was also prepared by dissolving 1.52g of thiourea in 100ml of distilled water and a solution of 1 M ammonium nitrate was obtained by dissolving 8.0 g of ammonium nitrate in 100 ml of distilled water. Indium nitrate solution, ammonium nitrate solution, thiourea solution and cadmium nitrate solution were added one by one to the precursor solution and each had a volume of 10 ml. The mixture was stirred continuously with the help of magnetic stirrer to make it homogeneous. Four different samples were prepared by adding at different concentration of indium nitrate solution, which are 0.005 M, 0.007 M, 0.009 M and 0.011 M to investigate the effect of indium doping concentration. These samples were designated SA, SB, SC and SD. The final pH of the solution was adjusted between 9 to11 using ammonium hydroxide to make the appropriate conditions for the formation of CdS thin film.

For the film deposition, about 0.2ml of CdS:In solution was dropped onto the centre of each substrate. The spin coating process was carried out at a speed of 4000 rpm for 60 seconds. This enabled the solution to be spread evenly over the surface of the substrate and a thin layer to be formed by evaporation of the solvent. The coated substrates were then removed and dried to obtain uniform indium doped cadmium sulfide thin films for further characterization and analysis.

RESULTS AND DISCUSSION

Structural characterization

A diffractometer was employed, scanning at a rate of 2 degrees per minute over a range of 10 to 100 degrees using CuKα radiation (with a wavelength of 1.5406 Å) set at 40 kV and 20 mA to analyze the structure. Figure 3.1 (a-d) shows the X-ray diffraction (XRD) pattern for a CdS:In film. The distinct and prominent peaks represent different crystalline planes, which possess various orientations. The XRD pattern exhibit major diffraction peaks at 26.55°, 33.75°, 37.80, 51.70°, and 68.80° which corresponds to (002), (101), (102), (110) and (112) crystal planes, respectively. XRD pattern compares well with JCPDS data (JCPDS No: 41-1049) of pure hexagonal CdS:In. (Yang et al., 2019). The table 3.1 shows the summary of the calculated crystal size from the major peaks among the 4 samples.

Table 3.1 summary of the calculated crystal size from the major peaks.

Peak	Experimental 2θ (°)	Assigned plane	FWHM (°)	FWHM (rad)	Crystallite size, D (nm)
1	26.55	-2	0.6445	0.01125	12.67
2	33.75	-101	0.6219	0.01085	13.35
3	37.8	-102	0.6007	0.01049	13.98
4	51.7	-112	0.6409	0.01119	13.77

Average size of the crystallite in CdS:In crystals is determined by Scherrer formula,

$$D = K\lambda/\beta\cos\theta \qquad 4.1$$

In this case D refers to the grain size, K is a constant set to 0.9, β is the full width at half maximum (FWHM) in radians and λ is the wavelength of the x-rays. The width of the XRD has been used to determine the sizes of the crystallites as 12.67 nm to 13.77 nm of the CdS films. Mean size of crystallite as obtained after XRD pattern analysis is D = 13.44 nm. Figure 3.1 (a)-(d) presents an X-ray diffraction (XRD) pattern for four samples that were created using varying concentrations of indium.

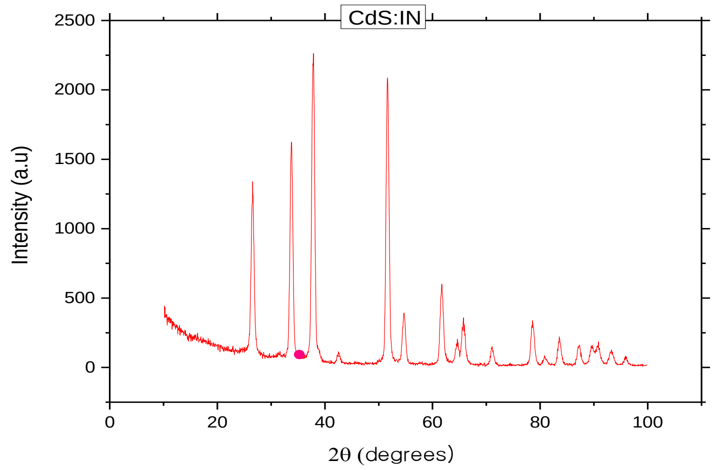

Figure 3.1(a) X ray diffraction pattern of CdS;In film sample SA

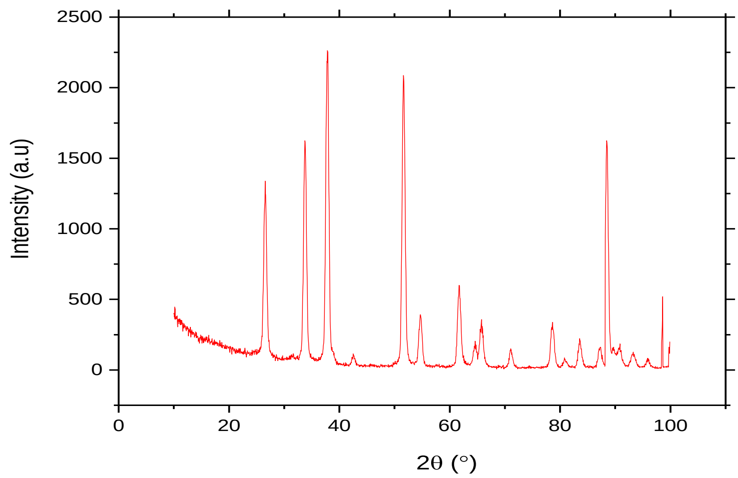

Figure 3.1 (b) X ray diffraction pattern of CdS;In film sample SB

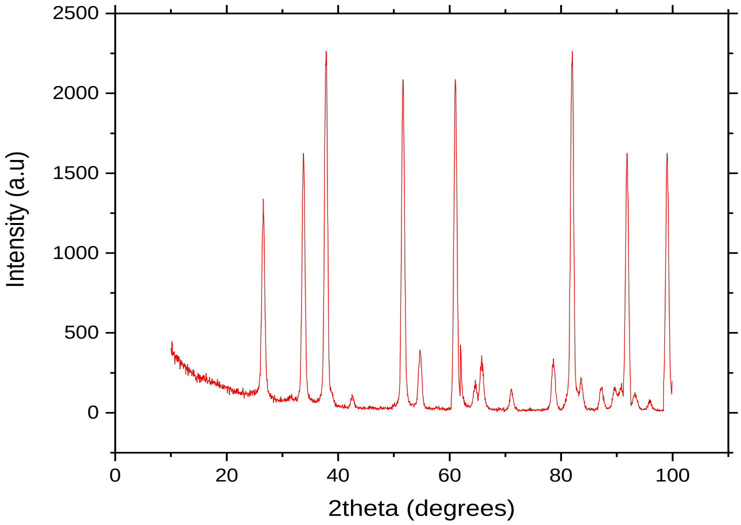

Figure 3.1(c) X ray diffraction pattern of CdS;In film sample SC

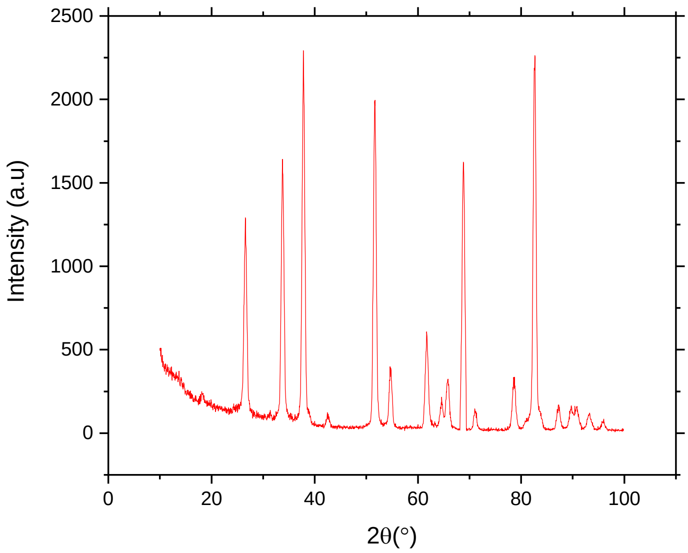

Figure 3.1 (d) X ray diffraction pattern for sample S_D

The clear peaks observed confirm the successful creation of indium-doped cadmium sulfide structures, as these peaks correspond to particular planes within the crystal lattice. The formation of the CdS: In structures is evidenced by distinct peaks linked to specific crystalline planes. A higher intensity of peaks indicates a more significant level of crystallinity, and the definition of these peaks also serves as a measure of the degree of crystallinity. Nearly all the peaks across samples with indium concentrations of 0.005M, 0.007M, 0.009M, and 0.011M reflect comparable diffraction patterns, suggesting that these samples may share a similar crystalline phase. This indicates that altering the dopant concentration had no effect on the crystalline structure of the CdS:In thin films. The prominence of the peaks is due to heightened crystallinity, and the sharpness of these peaks further suggests the extent of crystallinity. Almost all the peaks found in samples with varying indium concentrations of 0.005 M, 0.007 M, 0.009 M, and 0.011 M exhibit comparable diffraction patterns, implying that they likely possess a similar crystalline phase. This demonstrates that the variation in concentration did not modify the crystal structure of cadmium sulfide. Higher intensity peaks correspond to higher crystallinity, which is preferred because device stability is highly dependent on the crystallinity of the thin film (Islam et al., 2020) A higher crystallinity of the film can also lead to minimized defect states and charge recombination, hence improved device efficiency (Dharmadasa & Alam, 2022). It can be concluded that a higher doping level promotes crystal growth, as the concentration of the doping is increased from SA to SC, a progressive improvement in the crystal growth is observed, with the increase in intensity of the diffraction peaks. This implies that the crystallinity is enhanced by increasing the indium concentration up to 0.009M (sample SC). But when the concentration is above this optimum concentration as observed in sample SD (0.011M), the trend is reversed. Despite the higher doping level, a small decrease in the peak intensity is seen, which signifies that the lattice distortion and surface roughness has begun to increase. This means that as the amount of indium is increased, the crystal structure is damaged, and the crystallinity of the film is lowered.

Morphological characterization

The surface morphology of CdS:In thin films was examined using a Scanning Electron Microscope (SEM) to assess their suitability for photovoltaic (PV) applications. Figure 4.6(a)-(c) shows a SEM micro graph of CdS:In. Figures 3.2 (a), (b), and (c), display the morphological analysis of the samples SB, SC and SD taken at a 20,000 X magnification. The film crystals and sizes are equally and evenly distributed. All the three top view SEM images displayed hexagonal shaped crystallites and did not display a significant difference in crystal size

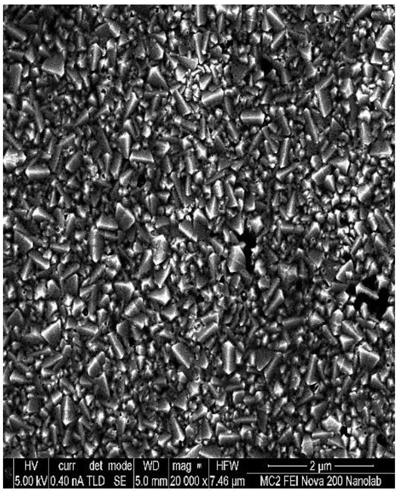

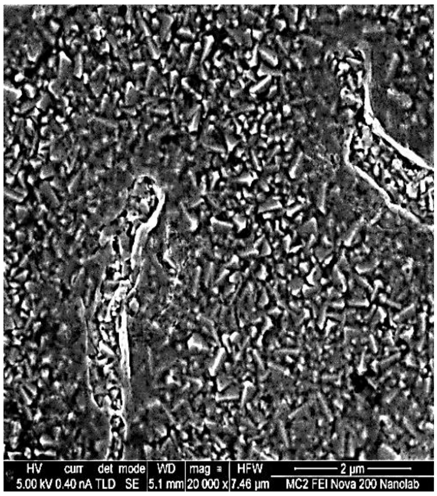

Figure 3.2 (a) Figure 3.2 (b) Figure 3.2 (c)

Figure 3.2 SEM micro graph of CdS;In thin film for sample SB, SC and SD..

From Figure 3.2 (a), it is observed that the layer with a concentration of 0.007M exhibits incomplete surface coverage with its grain structure. The surface also appears to be comparably uneven and likely thicker, which may increase the chances of agglomeration. In Figure 3.2 (b), produced at a concentration of 0.009M, the layer's surface is seen to be somewhat smoother and more consolidated than the film created with a concentration of 0.007M. Its crystalline structures look more polished with fewer noticeable gaps. This improvement might result from better crystal growth and enhanced uniformity of the surface. As In3+ ions replace Cd2+ ions, the growth process is influenced by diminishing excessive nucleation and encouraging the development of larger, tightly arranged grains. Consequently, this enhances the mobility of atoms on the surface, allowing for a more even settling of atoms and the filling of gaps, which leads to a denser, well-packed, and smooth film. Nevertheless, certain areas within this layer indicate particle clustering, with large aggregates irregularly scattered, as shown in Figure 3.2 (b). Sample SD demonstrates a rougher texture compared to sample SC, even though it has a higher concentration than the latter. This is attributed to the fact that the smoothing effect generally takes place only up to a certain optimal doping level. Beyond this point, an excess of indium can result in lattice distortions, causing the formation of secondary phases, which subsequently results in a rougher texture again. In solar cells, smoother surfaces facilitate better charge transport and ultimately lower charge recombination by minimizing leakage current (Mo et al., 2025). Therefore, attaining a smooth surface on thin films is essential. A consistent surface coverage combined with larger grain sizes can potentially lead to enhanced efficiency in manufactured solar cells by reducing recombination at the grain boundaries (Sherkar et al., 2017). Among the three samples analyzed in this research, the layer with a concentration of 0.007M was regarded as the most advantageous as it exhibited a smoother surface.

CONCLUSIONS

This study successfully investigated CdS: In thin films fabricated using the spin coating technique, demonstrating its effectiveness in producing uniform, high-quality films suitable for photovoltaic applications. Structural analysis confirmed that CdS: In films possess a hexagonal structure, The CdS: In layers display high intensity peaks corresponding to good crystallinity. The intensity of peaks increased with increase in indium doping. The morphological analysis of the CdS: In films shows incomplete surface coverage. However, the surface of sample SC layer appears smoother and more uniform, suggesting that higher doping levels result in smoother, more uniform thin films. Smoother films contribute to the efficiency of a solar cell making it a favorable layer in thin film photovoltaic cells fabrication. At high doping levels, morphological investigation showed well-dispersed grains and better surface consistency that is vital to minimize recombination losses in solar panels.

ACKNOWLEDGEMENT

The Electronics Research Laboratory, Physics Department, of Egerton University provided the Spin coater and magnetic stearer that were instrumental during deposition of thin films. The University of Michigan's Center for Complex Particle Systems grant an access to the XRD and SEM facilities that are utilized for the structural and morphological characterization of the thin films. The authors sincerely appreciate the technical assistance provided during the structural measurements and access to this facility.

CONFLICT OF INTEREST

The authors declare that there is no conflict of interest.

Credit Authorship Contribution Statement

John Ogana Ogechi: Writing original draft, Methodology, Investigation, Formal analysis.

Daniel Ketui: Writing review & editing, Supervision, Methodology, Conceptualization.

Duke Oeba: Writing review & editing, Supervision, Methodology, Conceptualization

REFERENCES

1. Arun, A. P., Sreenivasan, N., Patil, J. H., Kusanur, R., Ramachandraiah, H. L., & Ramakrishna, M. (2025). Thin films for next generation technologies: A comprehensive review of fundamentals, growth, deposition strategies, applications, and emerging frontiers. Processes, 13(12), 3846.
2. Belaid, W., Gezgin, S. Y., Basyooni-M. Kabatas, M. A., Eker, Y. R., & Kiliç, H. Ş. (2024). Utilizing gold nanoparticle decoration for enhanced UV photodetection in CdS thin films fabricated by pulsed laser deposition: Exploiting plasmon-induced effects. Nanomaterials, 14(5), 416.
3. Das, N., Chakrabartty, J., Farhad, S., Gupta, A. S., Ahamed, E. I., Rahman, K., Wafi, A., Alkahtani, A., Matin, M., & Amin, N. (2020). Effect of substrate temperature on the properties of RF sputtered CdS thin films for solar cell applications. Results in Physics, 17, 103132.
4. Deshmukh, S., Kheraj, V., & Panchal, A. (2018). Preparation of nanocrystalline CdS thin film by successive ionic layer adsorption and reaction (SILAR) method. Materials Today: Proceedings, 5(10), 21322–21327.
5. Dharmadasa, I., & Alam, A. (2022). How to achieve efficiencies beyond 22.1% for CdTe-based thin-film solar cells. Energies, 15(24), 9510.
6. Dong, X., Deng, W., Zhi, Y., Shen, B., Li, S., Tang, C., Lu, M., Jiang, S., Qiu, J., & Li, L. (2026). Heterojunction interface cation substitution to enhance the performance of antimony selenide thin-film solar cells. Energy Materials, 6(3), N-A.

7. Hossain, S. S., Tarek, M., Munusamy, T. D., Karim, K. M. R., Roopan, S. M., Sarkar, S. M., Cheng, C. K., & Khan, M. M. R. (2020). Facile synthesis of CuO/CdS heterostructure photocatalyst for the effective degradation of dye under visible light. Environmental Research, 188, 109803.
8. Huang, Y., Feng, L., Yang, J., Wang, H., Yu, Z., Guo, H., Yin, Y., Zhang, H., Li, Z., & Yan, J. (2026). Close-Spaced Sublimation of CdCl2 Enables Uniform CdS Thin Films for Certified 8.08%-Efficient Sb2S3 Solar Cells. Advanced Materials, 38(11), e20937.
9. Islam, S., Hossain, T., Sarwar, H., & Rashid, M. J. (2020). A systematic study on chemically deposited cadmium sulfide (CdS) thin film. Journal of Theoretical and Applied Physics, 14(3), 265–274.
10. Johnson, R. W., Hultqvist, A., & Bent, S. F. (2014). A brief review of atomic layer deposition: From fundamentals to applications. Materials Today, 17(5), 236–246.
11. Jothika, B., Rajamanickam, G., & Chauhan, A. (2025). Enhancing performance of hole transport layer-free carbon-based organic-inorganic halide perovskite solar cells with tuning guanidinium thiocyanate through additive engineering. Optical Materials, 160, 116758.
12. Kumar, S. G., & Rao, K. K. (2013). Physics and chemistry of CdTe/CdS thin film heterojunction photovoltaic devices: Fundamental and critical aspects. Energy & Environmental Science, 7(1), 45–102.
13. Kumar, V., Sharma, D., Bansal, M., Dwivedi, D., & Sharma, T. (2011). Synthesis and characterization of screen-printed CdS films. Science of Sintering, 43(3), 335–341.
14. Kumari, S., Chasta, G., Suthar, D., Kumari, N., & Dhaka, M. (2025). Understanding grain growth and grain boundary inversion in CdS thin films by CdI2 activation. Thin Solid Films, 811, 140593.
15. Lakmal, A., Kumarasinghe, R., Seneviratne, V., Chen, J.-Y., Song, J.-M., & Dassanayake, B. (2021). Thermally evaporated CdS thin films for CdS/CdTe solar cells: Effect of substrate temperature on CdS layer. Materials Science and Engineering: B, 273, 115406.
16. Li, K., Cai, Z., Yang, J., Wang, H., Zhang, L., Tang, R., Zhu, C., & Chen, T. (2023). Molecular beam epitaxy deposition of in situ O-doped CdS films for highly efficient Sb2 (S, Se) 3 solar cells. Advanced Functional Materials, 33(48), 2304141.
17. Luo, G., Ren, X., Zhang, S., Wu, H., Choy, W. C., He, Z., & Cao, Y. (2016). Recent advances in organic photovoltaics: Device structure and optical engineering optimization on the nanoscale. Small, 12(12), 1547–1571.
18. Madhavi, J., & Prasad, V. (2020). ZnS and ZnS/CdS core-shell Nano particles: Synthesis, properties and Perspectives. Surfaces and Interfaces, 21, 100757.
19. Mo, Y., Li, C., Yang, J., Wang, X., Hu, P., Chen, X., Chen, T., Xiao, X., & Li, J. (2025). High-Efficiency All-Antimony Chalcogenide Tandem Solar Cells via Thermal-Evaporated CdS Interface Engineering. Advanced Materials, 37(40), e06372.
20. Raza, Z. (2025). 4 1D nanomaterials and. Nanostructured Materials for Energy Applications, 111.
21. Sen, S. K., Paul, T. C., Dutta, S., Hossain, M., & Mia, M. N. H. (2020). XRD peak profile and optical properties analysis of Ag-doped h-MoO3 nanorods synthesized via hydrothermal method. Journal of Materials Science: Materials in Electronics, 31(2), 1768–1786.
22. Sherkar, T. S., Momblona, C., Gil-Escrig, L., Ávila, J., Sessolo, M., Bolink, H. J., & Koster, L. J. A. (2017). Recombination in perovskite solar cells: Significance of grain boundaries, interface traps, and defect ions. ACS Energy Letters, 2(5), 1214–1222.
23. Shkir, M., Anis, M., Shaikh, S., & AlFaify, S. (2019). An investigation on structural, morphological, optical and third order nonlinear properties of facilely spray pyrolysis fabricated In: CdS thin films. Superlattices and Microstructures, 133, 106202.
24. Shkir, M., Ashraf, I., Khan, A., Khan, M. T., El-Toni, A. M., & AlFaify, S. (2020). A facile spray pyrolysis fabrication of Sm: CdS thin films for high-performance photodetector applications. Sensors and Actuators A: Physical, 306, 111952.
25. Wahab, A., Tofil, H. M., Rahman, G., Nguyen, D. L. T., Shah, A. ul H. A., & Joo, O. S. (2026). Cadmium Sulfide-Based Nanostructures for Next-Generation Multifunctional Applications: Design Strategies, Decoding Performance Limitations, and Recent Advances. ChemCatChem, 18(11), e70837.
26. Wilson, G. M., Al-Jassim, M., Metzger, W. K., Glunz, S. W., Verlinden, P., Xiong, G., Mansfield, L. M., Stanbery, B. J., Zhu, K., & Yan, Y. (2020). The 2020 photovoltaic technologies roadmap. Journal of Physics D: Applied Physics, 53(49), 493001.

27. Xu, Y., Li, G., Li, R., Jing, Y., Zhang, H., Wang, X., Du, Z., Wu, J., & Lan, Z. (2022). PbS/CdS heterojunction thin layer affords high-performance carbon-based all-inorganic solar cells. Nano Energy, 95, 106973.
28. Yang, X., Wang, B., Mu, Y., Zheng, M., & Wang, Y. (2019). Photocatalytic performance of cubic and hexagonal phase CdS synthesized via different Cd sources. Journal of Electronic Materials, 48, 2895–2901.
29. Yasin, S., Waar, Z. A., Christopoulos, S., & Moustafa, M. (2026). In-Depth Numerical Evaluation and Performance Optimization of Cmts Photodetector. Ukrainian Journal of Physical Optics, 27(2), 02058–02069.